Enzymatic characteristics of D-mannose 2-epimerase, a new member of the acylglucosamine 2-epimerase superfamily

Wataru Saburi,[1,*] Suzuka Sato,[1] Saki Hashiguchi,[1] Hirohiko Muto,[1] Takahisa Iizuka,[2] and Haruhide Mori[1,*]

[1]*Research Faculty of Agriculture, Hokkaido University, Kita 9, Nishi 9, Kita-ku, Sapporo 060-8589, Japan*

[2]*Nihon Shokuhin Kako Co., Ltd., 30 Tajima, Fuji, Shizuoka 417-8530, Japan*

*Corresponding authors. Tel/Fax: +81-11-706-2508; E-mail: saburiw@chem.agr.hokudai.ac.jp (W. Saburi). Tel/Fax: +81-11-706-2497; E-mail: hmori@chem.agr.hokudai.ac.jp (H. Mori).

Abstract

Carbohydrate epimerases and isomerases are essential for the metabolism and synthesis of carbohydrates. In this study, *Runella slithyformis* Runsl_4512 and *Dyadobacter fermentans* Dfer_5652 were characterized from a cluster of uncharacterized proteins of the acylglucosamine 2-epimerase (AGE) superfamily. These proteins catalyzed the intramolecular conversion of D-mannose to D-glucose, whereas they did not act on β-(1→4)-mannobiose, *N*-acetyl-D-glucosamine, and D-fructose, which are substrates of known AGE superfamily members. The k_{cat}/K_m values of Runsl_4512 and Dfer_5652 for D-mannose epimerization were 3.89 and 3.51 $min^{-1}mM^{-1}$, respectively. Monitoring the Runsl_4512 reaction through ^{1}H-NMR showed the formation of β-D-glucose and β-D-mannose from D-mannose and D-glucose, respectively. In the reaction with β-D-glucose, β-D-mannose was produced at the initial stage of the reaction, but not in the reaction with α-D-glucose. These results indicate that Runsl_4512 catalyzed the 2-epimerization of the β-anomer substrate with a net retention of the anomeric configuration. Since ^{2}H was obviously detected at the 2-C position of D-mannose and D-glucose in the equilibrated reaction mixture produced by Runsl_4512 in $^{2}H_2O$, this enzyme abstracts 2-H from the substrate and adds another proton to the intermediate. This mechanism is in accordance with the mechanism proposed for the reactions of other epimerases of the AGE superfamily, that is, AGE and cellobiose 2-epimerase. Upon reaction with 500 g/L D-glucose at 50°C and pH 8.0, Runsl_4512 and Dfer_5652 produced D-mannose with a 24.4 and 22.8% yield, respectively. These D-mannose yields are higher than those of other enzyme systems, and ME acts as an efficient biocatalyst for producing D-mannose.

Keywords: D-mannose; epimerase; cellobiose 2-epimerase; acylglucosamine 2-epimerase; D-mannose

isomerase

Introduction

Carbohydrates are the most abundant organic compounds in nature; they have diverse structures due to presence of various monosaccharide units, linkages, and degrees of polymerization. To metabolize carbohydrates, organisms utilize several intra- and extracellular enzymes, such as glycoside hydrolases, glycoside phosphorylases, and sugar isomerases/epimerases. Moreover, these metabolizing enzymes have great potential for application in carbohydrate synthesis. As only few carbohydrate types, including starch, sucrose, and lactose, are abundantly available, enzymatic conversion of abundant sugars to rare sugars is required to utilize rare sugars as foodstuffs and drags.

Carbohydrate isomerases and epimerases catalyze the isomerization (conversion between aldose and ketose) and epimerization (conversion between epimers) of carbohydrates, respectively. These enzymes are essential in major carbohydrate metabolic pathways including glycolysis, oxidative/reductive pentose phosphate pathways, and Leloir pathway, and provide suitable reactions for carbohydrate conversions. For instance, isomerization of D-glucose to D-fructose by D-xylose isomerase (EC 5.3.1.5) is widely applicable in the production of D-fructose-rich syrup (Bhosale et al. 1996). Furthermore, D-xylose isomerase facilitates biofuel production from lignocellulosic biomass (Kuyper et al. 2004). Cellobiose 2-epimerase (CE; EC 5.1.3.11) produces epilactose [β-D-galactopyranosyl-(1→4)-D-mannose] from lactose via 2-epimerization of reducing end sugar residue (Ito et al. 2008; Saburi et al. 2010). This disaccharide has a prebiotic property (Watanabe et al. 2008) and enhances mineral absorption (Nishimukai et al. 2008;

Suzuki et al. 2010a; Suzuki et al. 2010b) and energy expenditure in the skeletal muscle and brown adipose tissues in order to avoid obesity (Murakami et al. 2015). D-Tagatose 3-epimerase (EC 5.1.3.31) isomerizes D-fructose to produce D-psicose (Takeshita et al. 2000). D-Psicose is not metabolized by humans (Iida et al. 2010) and exhibits antiobesity activity by increasing the energy expenditure (Ochiai et al. 2013; Ochiai et al. 2014). UDP-galactose 4-epimerase (EC 5.1.3.2) is applied to the enzymatic production of lacto-*N*-biose I [β-D-galactopyranosyl-(1→3)-*N*-acetyl-D-glucosamine], which is a part of type I human milk oligosaccharide and has prebiotic property (Nishimoto et al. 2007; Kiyohara et al. 2009).

Acylglucosamine 2-epimerase (AGE) superfamily includes several carbohydrate epimerases and isomerases: AGE (EC 5.1.3.8) (Itoh et al. 2000; Lee et al. 2007), CE (Saburi 2016), D-mannose isomerase (MI; EC 5.3.1.7) (Kasumi et al. 2014; Saburi et al. 2018), and sulfoquinovose isomerase (SQI; EC 5.3.1.31) (Denger et al. 2014). These enzymes share an $(\alpha/\alpha)_6$-barrel folded catalytic domain (Itoh et al. 2000; Lee et al. 2007; Saburi et al. 2018; Fujiwara et al. 2013; Fujiwara et al. 2014; Itoh et al. 2008). Two catalytic His residues on 8th and 12th α-helices of the catalytic domain and several residues for substrate binding are completely conserved throughout the family. During epimerization of *N*-acetyl-D-glucosamine and D-glucose residue of β-(1→4)-disaccharides by AGE and CE, respectively, catalytic His on the 12th α-helix abstracts the axial proton from 2-C of the substrate as general base catalyst in order to generate the *cis*-endiolate intermediate, and His on the 8th α-helix donates the proton to the intermediate as general acid catalyst for producing the epimerized product (Lee et al. 2007; Fujiwara et al. 2014). During isomerization of D-mannose to D-fructose by MI, His on the 8th α-helix mediates intramolecular

proton transfer between 1-C and 2-C (Itoh et al. 2008; Saburi et al. 2018).

In this study, a new carbohydrate epimerase, D-mannose 2-epimerase (ME), which can catalyze the 2-epimerization of D-glucose and D-mannose, was found via the functional analysis of the *Runella slithyformis* Runsl_4512 and *Dyadobacter fermentans* Dfer_5652 proteins present in an uncharacterized cluster of AGE superfamily proteins (Fig. 1). Enzymatic properties of these enzymes and the mechanism, through which they produce D-mannose from D-glucose, are described.

Materials and methods

Phylogenetic analysis of AGE superfamily proteins

Multiple sequence alignment of AGE superfamily enzymes was conducted using MAFFT version 7 (Katoh et al. 2017), and a phylogenetic tree was prepared using all gap-free sites (69 amino acid residues) through the neighbor joining method. The phylogenetic tree was visualized using a Figtree program version 1.4.3 (http://tree.bio.ed.ac.uk/software/figtree/).

Preparation of expression plasmids

The genes, encoding Runsl_4512 and Dfer_5652 (Genbank numbers, AEI50834.1 and ACT96842.1) were amplified from the genomic DNA via PCR using Primestar HS DNA polymerase (Takara Bio, Kusatsu, Japan). The genomic DNA of *R. slithyformis* DSM19594 and *D. fermentans* ATCC700827 were purchased from Deutsche Sammlung von Mikroorganismen und Zellkulturen (Braunschweig, Germany) and the American Type Culture Collection (Manassas, VA, USA), respectively. The primer sequences are

listed in Table 1. Amplified PCR products were inserted into pET-23a vector (Novagen, Darmstadt, Germany) via the restriction endonuclease sites: *Nde*I and *Xho*I sites for *Runsl_4512*, and *Eco*RI and *Xho*I sites for *Dfer_5652*. The recombinant enzymes had extra eight residues, Leu-Glu-His-His-His-His-His-His, at the C-terminal, and Dfer_5652 also had 16 residues, Met-Ala-Ser-Met-Thr-Gly-Gly-Gln-Gln-Met-Gly-Arg-Gly-Ser-Glu-Phe at the N-terminal. The DNA sequences of the insert and its flanking regions were verified by sequence analysis using an Applied Biosystems 3130 Genetic Analyzer (Life Technologies, Carlsbad, CA, USA).

Preparation of recombinant enzymes

Recombinant Runsl_4512 and Dfer_5652 were produced in transformant of *Escherichia coli* BL21 (DE3) carrying their expression plasmids. The transformants were grown in LB medium containing 100 μg/mL ampicillin, at 37 °C (1 L for Runsl_4512 and 6 L for Dfer_5652). Recombinant proteins were produced by adding 0.1 M isopropyl β-D-thiogalactopyranoside to a final concentration of 0.1 mM for Runsl_4512 and 0.05 mM for Dfer_5652, when absorbance at 600 nm reached 0.5. The induction was carried out at 18 °C for 20 h for Runsl_4512, and at 37 °C for 4 h for Dfer_5652. Bacterial cells, harvested via centrifugation at 6000 × *g* at 4 °C for 10 min, were suspended in 40 mL of 30 mM imidazole-HCl buffer containing 0.5 M NaCl (pH 7.0; buffer A) for Runsl_4512 and 30 mM imidazole-HCl buffer containing 0.3 M NaCl (pH 8.0; buffer B) for Dfer_5652. The cells were disrupted by sonication, and cell debris was removed via centrifugation at 18,000 × *g* at 4 °C for 10 min. The cell-free extract obtained was applied onto a Ni^{2+}-immobilized Chelating Sepharose Fast Flow column (2.8 cm i.d.

× 3.0 cm, GE Healthcare, Uppsala, Sweden) equilibrated with buffer A and B for Runsl_4512 and Dfer_5652, respectively. The column was washed with the starting buffer, and the adsorbed protein was eluted in a 30 to 500 mM linear gradient of imidazole (total elution volume, 200 mL). The fractions containing highly purified protein, as demonstrated by SDS-PAGE, were pooled and dialyzed against a 10 mM Tris-HCl buffer (pH 7.0). The sample was concentrated to 4–10 mg/mL via ultrafiltration using Vivaspin 20 centrifugal concentrators (nominal molecular weight limit 30,000 Da; Sartorius, Göttingen, Germany). Runsl_4512 was stored at −20 °C in the presence of 50% (v/v) glycerol. Dfer_5652 was stored at 4 °C without glycerol because this enzyme was fully stable under these conditions. Molar concentrations of the purified enzymes were determined to be the average of the protein concentrations, calculated, using Eq. 1, from the number of respective amino acids in one protein molecule and the concentrations of respective amino acids after acid hydrolysis of the purified enzyme in 6 M HCl at 110 °C for 24 h.

Eq. 1: Protein concentration (μM) = [amino acid concentration, μM]/number of amino acid

Amino acid concentrations were measured using a JLC-500/V amino acid analyzer (JEOL, Tokyo, Japan).

D187N mutation in Runsl_4512 was introduced with a Primestar Mutagenesis Basal Kit (Takara Bio). The expression plasmid of Runsl_4512 as template and primers, as listed in Table 1, were used. The mutant enzyme was prepared in a similar manner as the wild type.

Blue native PAGE

The purified Runsl_4512 and Dfer_5652 were evaluated by using blue native PAGE (BN-PAGE) (Schägger et al. 1994). The analytical sample was prepared using a Native PAGE Sample Prep Kit (Life Technologies). Native PAGE Novex 4– 16% Bio-Tris Gels (Life Technologies) were used and electrophoresis was performed at a constant 150 V for 115 min on ice. Native Mark Unstained Standard (Life Technologies) was used as protein molecular size standards.

Screening of substrates

Activity of various substrates was examined via TLC and high-performance anion exchange chromatography with pulsed amperometric detection (HPAEC-PAD). For TLC analysis, a reaction mixture (5 μL), containing 0.68–0.83 μM enzyme, 50 mM substrate [D-lyxose, D-mannose, D-glucose, D-tagatose, D-xylose (Wako Pure Chemical Industries, Osaka, Japan); D-talose, D-xylulose (Sigma, St. Louis, MO, USA); D-fructose, D-galactose (Nacalai Tesque, Kyoto, Japan); β-(1→4)-mannobiose, prepared as described previously (Kawahara et al. 2012)], and 5 mM Tris-HCl buffer (pH 8.0), was incubated at 37 °C for 4 h. About 1 μL of the sample was spotted on a silica gel plate (TLC Silica gel 60 F_{254} Aluminium sheet, Merck, Darmstadt, Germany) and developed by 2-propanose/1-butanol/water (2/2/1, v/v/v). Sugars were detected by spraying a detection reagent [acetic acid/sulfuric acid/anisaldehyde (100/2/1, v/v/v)] onto the plate, followed by heating of the plate. For HPAEC-PAD analysis, a reaction mixture (50 μL), containing 0.87–1.37 μM enzyme, 50 mM substrate [*N*-acetyl-D-glucosamine (Nacalai Tesque); *N*-acetyl-D-mannosamine, D-glucosamine (Tokyo Chemical Industry, Tokyo, Japan); and D-mannosamine (Wako Pure Chemical Industries)], and 40 mM HEPES-NaOH buffer

(pH 8.0), was incubated at 37 °C for 12 h. The reaction mixture was analyzed using HPAEC-PAD under following conditions: injection volume, 10 μL (10-fold diluted sample with water); column, Carbopac PA1 (4 mm i.d. × 250 mm; Thermo Fischer Scientific, Waltham, MA, USA); eluent, 18 mM NaOH; flow rate, 1 mL/min.

ME activity assay

The activity of epimerization to D-mannose was measured. A reaction mixture (100 μL) containing enzyme, 10 mM D-mannose, and 40 mM HEPES-NaOH (pH 8.0) was incubated at 37 °C for 20 min. The enzyme reaction was stopped by heating at 80 °C for 3 min, and 50 μL of the supernatant, obtained by centrifuging the reaction mixture at 13,000 × *g* at 4 °C for 5 min, was mixed with 50 μL of a mixture comprising 1 mM thio-NAD^+ (Wako Pure Chemical Industries), 2 U/mL hexokinase (Nacalai Tesque), 2 U/mL glucose 6-phosphate dehydrogenase (Nacalai Tesque), 14 mM ATP (Sigma), 0.2 M Tris-HCl buffer (pH 7.5), and 20 mM $MgCl_2$. This solution was incubated at 37 °C for 20 min, and its absorbance at 405 nm was measured. As a standard, 0–100 μM D-glucose containing 10 mM D-mannose was used. One unit (U) of enzyme activity was defined as an enzyme amount producing 1 μmol of D-mannose in 1 min under these conditions.

Kinetic parameters for the epimerization of D-mannose were determined from the reaction rates as 4–100 mM D-mannose. The Michaelis–Menten equation was fitted to the reaction rates by nonlinear regression using the Grafit ver. 7.0.2 software (Erithacus Software, East Grinstead, UK).

Assaying the epimerization activity of D-mannose 6-phosphate

A reaction mixture (200 μL), containing enzyme, 10 mM D-mannose 6-phosphate disodium salt (Sigma), and 40 mM HEPES-NaOH buffer (pH 8.0), was incubated at 37 °C for 30 min. Fifty μL of the reaction mixture was collected every 10 min and heated at 100 °C for 3 min to stop the reaction. D-Glucose 6-phosphate was quantified as follows: 50 μL of the sample was mixed with 20 μL of mixture containing 2.5 mM thio-NAD^+ and 5 U/mL D-glucose 6-phosphate dehydrogenase, and was then incubated at 37 °C for 30 min. Absorbance at 405 nm was measured, and D-glucose 6-phosphate concentration was calculated from a standard curve of D-glucose 6-phosphate disodium salt (0–250 μM; Oriental Yeast, Tokyo, Japan).

Effects of pH and temperature on activity and stability

Optimum pH was determined from the activities at various pH values. The pH of the reaction was varied using 100 mM Britton–Robinson buffer (pH 4.0–11.0) as reaction buffer. Optimum temperature was evaluated based on the activity at 20–70 °C. Residual activities after the pH and heat treatments were measured to evaluate the enzyme stability. During the pH treatment, the enzyme solution was incubated at pH 2.3–12.1 using 50 mM Britton–Robinson buffer at 4 °C for 24 h; whereas, during the heat treatment, the enzyme solution was incubated at 20–100 °C for 20 min. The pH and temperature ranges, in which the enzyme retained more than 90% of its original activity, were regarded as stable ranges.

Production of D-mannose from D-glucose

A reaction mixture (1 mL) containing 500 g/L D-glucose, 0.25 U/mL Runsl_4512 or Dfer_5652, and 50 mM HEPES-NaOH (pH 8.0) was incubated at 50 °C for 48 h. One hundred μL of the reaction mixture was collected at a stipulated time, diluted with water 10 times, and heated at 100 °C for 5 min to stop the reaction. The sugar content of the reaction mixture was analyzed via HPLC under the following conditions: sample injection volume, 10 μL; column, Hilic Pac VG50 4E (4.6 mm i.d. × 250 mm; Shodex, Tokyo, Japan); column temperature, 40 °C; eluent, 80% (v/v) acetonitrile; flow rate, 0.6 mL/min; and detection, refractive index. Authentic D-glucose, D-mannose, and D-fructose were used as standards.

NMR analysis of the reaction products of Runsl_4512

The epimerization of D-mannose and D-glucose by Runsl_4512 was monitored by ^{1}H-NMR. H_2O in the enzyme solution was replaced with $^{2}H_2O$: the enzyme solution was diluted with 10 mM HEPES-$NaO^{2}H$ buffer in $^{2}H_2O$ ($p^{2}H$ 8.0) by 3-fold and was further concentrated to the original volume via ultrafiltration as aforementioned. These steps were repeated four times in total. ^{1}H-NMR of a reaction mixture (0.5 mL), containing Runsl_4512 (23 and 73 μM for the reactions with D-mannose and D-glucose, respectively), 250 mM substrate, and 10 mM HEPES-Na buffer ($p^{2}H$ 8.0), was recorded at 27 °C using Bruker AMX500 (Billerica, MA, USA). In the reactions with D-glucose and D-mannose, 22.5 mg of substrate powder was dissolved in 50 μL of $^{2}H_2O$ and incubated at 25 °C for 24 h to obtain the equilibrium mixture of α- and β-anomers. This substrate solution was mixed with 450 μL of the enzyme solution in 10 mM HEPES-$NaO^{2}H$ buffer ($p^{2}H$ 8.0), and this mixture was immediately subjected to the ^{1}H-NMR analysis. In the reactions with α-D-glucose (Sigma) and β-D-glucose (Sigma), 22.5 mg of sugar

was dissolved with 0.5 mL of the enzyme solution in 10 mM HEPES-NaO^{2}H buffer (p^{2}H 8.0) just before the reactions.

The reaction mixture with D-mannose was incubated at 25 °C for 24 h to prepare an equilibrium reaction mixture. ^{1}H-NMR of this mixture was recorded, and the spectrum was compared with the equimolar mixture (250 mM) of D-glucose and D-mannose. This reaction mixture was dried up under reduced pressure, and the residue was dissolved in H_2O. ^{2}H-NMR was recorded to detect ^{2}H in the reaction products.

Results

Determination of catalytic activity of Runsl_4512 and Dfer_5652

Runsl_4512 and Dfer_5652, belonging to a cluster of uncharacterized proteins in a phylogenetic analysis of AGE superfamily enzymes (Fig. 1), were emphasized in this study. The amino acid sequence of Runsl_4512 is 74% identical with that of Dfer_5652, and sequence identities of Runsl_4512 and Dfer_5652 with characterized AGE superfamily members are as follows: *Ruminococcus albus* CE, 24% and 24%; *Rhodothermus marinus* CE, 25% and 25%; *Anabaena* sp. AGE, 16% and 17%; *E. coli* SQI, 14% and 13%; *Marinomonas mediterranea* MI, 18% and 19%; and *Thermobifida fusca* MI, 12% and 17%, respectively.

To investigate the enzymatic functions of Runsl_4512 and Dfer_5652, recombinant enzymes were produced in *E. coli* transformant, and purified. These proteins were displayed as single bands on SDS-PAGE and BN-PAGE (Fig. 2). The molecular masses of Runsl_4512 and Dfer_5652 were estimated to be

45 kDa (theoretical molecular mass, 50 kDa) and 47 kDa (theoretical molecular mass, 52 kDa) on SDS-PAGE, and 81 kDa and 101 kDa on BN-PAGE, respectively. These results suggested that Runsl_4512 and Dfer_5652 exist as homodimers under nondenaturing conditions. The purified samples were then incubated with various carbohydrates to find their substrates, and D-mannose and D-glucose were detected as the reaction products from D-glucose and D-mannose, respectively (Fig. 3). This result indicates that these proteins catalyzed the epimerization of D-mannose (ME reaction). No reaction products were detected in the reactions with D-galactose, D-talose, D-xylose, D-lyxose, D-glucosamine, D-mannosamine, *N*-acetyl-D-glucosamine, *N*-acetyl-D-mannosamine, β-(1→4)-mannobiose, D-mannose 6-phosphate, D-fructose, D-tagatose, and D-xylulose.

Enzymatic properties of Runsl_4512 and Dfer_5652 were investigated based on the ME activity. The ME activity at pH 4.0–11.0 was measured to evaluate the optimum pH. Runsl_4512 and Dfer_5652 were most active at pH 7.8 and 8.1, respectively. Optimum temperature was evaluated based on the activity at 20–70 °C. Both enzymes exhibited highest activity at 37 °C. Stable pH and temperature ranges of these enzymes were pH 6.3–10 (4 °C for 24 h) and at ≤40 °C (pH 8.0 for 20 min), respectively. The Michaelis–Menten equation fitted well with the reaction rates of Runsl_4512 and Dfer_5652 at various D-mannose concentrations (Fig. 4). The K_m values were determined from the concentration of D-mannose, including both α- and β-anomers. The k_{cat} and K_m of Runsl_4512 were 286 min^{-1} and 73.5 mM, and those of Dfer_5652 were 233 min^{-1} and 66.4 mM, respectively (Table 2).

Production of D-mannose from D-glucose

D-Mannose was enzymatically synthesized from 500 g/L D-glucose (Fig. 5). The concentrations of D-mannose reached 122 g/L and 114 g/L, 48-h after reaction with Runsl_4512 and Dfer_5652, respectively. Molar rates of conversion to D-mannose using Runsl_4512 and Dfer_5652 were 24.4% and 22.8%, respectively. Faint D-fructose production was observed: D-fructose concentrations after 48-h reactions with Runsl_4512 and Dfer_5652 were 8.5 and 7.9 g/L, respectively. These D-fructose concentrations were consistent with those observed after a 48-h reaction without enzyme 8.3 g/L. Thus, the D-fructose generated in ME reaction mixtures was regarded as a nonenzymatic reaction product. Nonenzymatic epimerization was not observed under the reaction conditions.

NMR analysis of the reaction products by Runsl_4512

The anomeric configuration of the products of reactions carried out using Runsl_4512 was analyzed through ^{1}H-NMR. In the reactions with D-mannose and D-glucose (equilibrium mixture of α- and β-forms), the 1-H signals of β-D-glucose (4.63 ppm) and β-D-mannose (4.88 ppm) were detected from the initial stage of the reactions whereas the 1-H signals of α-D-glucose (5.22 ppm) and α-D-mannose (5.18 ppm) were not (Fig. 6A and B). This result indicates that β-D-glucose and β-D-mannose were produced from D-mannose and D-glucose, respectively. Production of the epimerized product from α- and β-D-glucose was monitored (Fig. 6C and D). The 1-H signal of β-D-mannose was detected at the initial stage of the reaction with β-D-glucose, but in the reaction with α-D-glucose, this signal was scarce and was only observed in the later stages, along with the production of β-D-glucose. Thus, Runsl_4512 used β-D-glucose as the substrate.

The equilibrium reaction mixture, produced from D-mannose in $^{2}H_2O$, was analyzed by ^{1}H- and ^{2}H-NMR analyses (Fig. 6E). In the ^{1}H-NMR spectrum of the equilibrium reaction mixture, 2-H signals of D-mannose (3.9 ppm) and D-glucose (3.2 ppm and 3.5 ppm for β- and α-D-glucose, respectively) were not detected, whereas ^{2}H signals were clearly detected at the corresponding chemical shifts of the 2-H of D-mannose and D-glucose by ^{2}H-NMR. This result indicates that Runsl_4512 abstracts 2-H from the substrates and adds ^{2}H from the reaction solvent.

Site-directed mutagenesis at Asp187 of Runsl_4512

Multiple sequence alignment of AGE superfamily enzymes was carried out to compare the amino acid sequences of MEs with those of the other members (Fig. 7). His273 and His404 of Runsl_4512 and Dfer_5652 correspond to the catalytic His residues of known enzymes, which are situated on the 8th and 12th α-helices of the catalytic $(\alpha/\alpha)_6$-barrel domain. Arg60, Tyr119, His191, Glu276, and Trp336 of Runsl_4512 and Dfer_5652 also correspond to the substrate-binding residues of CE, MI, and SQI, which act on the substrates harboring 2-OH group. Nevertheless, in the ME sequences, Asp187 was observed as the equivalent residue of Asn on α-helix 6 of CE, MI, and SQI, which has a hydrogen bonding interaction with 2-OH of substrates (Fujiwara et al. 2014, Itoh et al. 2008). D187N mutant of Runsl_4512 was prepared to evaluate the importance of Asp187. The activity of this mutant enzyme to 10 mM D-mannose was not detectable (<0.002 U/mg), while that of wild type was 0.61 U/mg. Thus, Asp187 is essential for the catalytic activity of Runsl_4512.

Discussion

Carbohydrate epimerization and isomerization are essential reactions to convert abundant sugars into rare sugars. In this study, reversible 2-epimerization activity between D-mannose and D-glucose was observed in Runsl_4512 and Dfer_5652 proteins belonging to a yet uncharacterized protein cluster of AGE superfamily (Fig. 1). This activity was also detected in several CEs (Park et al. 2011; Saburi et al. 2015); however, the k_{cat}/K_m values of Runsl_4512 and Dfer_5652 were 4.1–140-fold higher than CEs from *Caldicellulosiruptor saccharolyticus* and *Cellvibrio vulgaris* (Table 2). In contrast to CEs, Runsl_4512 and Dfer_5652 did not present any detectable epimerization activity to β-(1→4)-linked disaccharides.

Sequence comparison between MEs and function-known AGE superfamily enzymes revealed that the MEs have residues corresponding to two catalytic His residues and a majority of residues important for substrate-binding in MI, SQI, and CE (Fig. 7); ME presumably shares the mechanisms of substrate binding and catalysis with these enzymes. Among the possible residues involved in the substrate binding, only Asp187 of Runsl_4512 and Dfer_5652 differs from the corresponding residue of CE and MI as aforementioned. As Asp187 was confirmed to be essential for the catalytic activity through D187N mutation in Runsl_4512, it might have specific function for ME activity. Multiple-sequence alignment suggests that ME has a longer loop connecting the 7th and 8th α-helices (α7→α8 loop) than any characterized AGE superfamily member (Fig. 7). In MI, the corresponding loop is predicted to cause steric hindrance upon binding to the disaccharide substrate (Saburi et al. 2018). Therefore, long α7→α8 loop of ME might be important for the monosaccharide specificity. Three-dimensional structure analysis

of MEs would provide essential information to understand the structure–function relationship of this enzyme.

Analysis of anomeric configuration of the reaction product by ^{1}H-NMR revealed that ME forms the product of β-anomer. This anomeric configuration of the reaction product is in accordance with that of β-(1→4)-disaccharides bound to CE (Fujiwara et al. 2014), and the isomerized product, D-mannose, from D-fructose by MI (Saburi et al. 2018). In the reaction with β-D-glucose, β-D-mannose was formed from the initial stage of the reaction; however, this was not observed in the reaction with α-D-glucose. Thus, ME utilizes β-glucose as a substrate, that is, the anomeric configuration of the substrate is retained in the product. Slight production of β-D-mannose in the later stage of the reaction with α-D-glucose is presumably attributable to the reaction with β-D-glucose, generated from α-D-glucose via mutarotation. Retention of β-anomer in the substrate and product is presumably suitable for the ring opening and closure mechanism catalyzed by His on the 12th α-helix as general acid/base catalyst, which forms hydrogen bonds with 1-O and 5-O of the substrate of β-anomer (Fujiwara et al. 2014).

The NMR analysis of the equilibrated reaction product indicated that 2-H of the substrate was substituted with ^{2}H from solvent $^{2}H_2O$, indicating that ME epimerizes the substrate via proton abstraction and addition mechanisms as postulated in CE and AGE (Lee et al. 2007; Fujiwara et al. 2014). Based on the sequence comparison between ME and CE, it is predicted that His273 of Runsl_4512 and Dfer_5652 serves as general base catalyst to abstract 2-H from D-mannose and produce *cis*-endiolate intermediate, and His404 serves as general acid catalyst to donate proton to the intermediate and produce D-glucose (Fig. 8).

D-Mannose has several beneficial physiological properties, such as preventing urinary tract infections (Kranjčec et al. 2014) and treating phosphomannose isomerase deficient induced congenital disorders of glycosylation (de Lonlay and Seta 2009), and it could be widely applied as an important intermediate for synthesizing immunostimulatory agents (Ranta et al. 2012), vitamin (Chen et al. 2007), and D-mannitol (Ghoreishi and Shahrestani 2009). Furthermore, D-mannose is useful as an animal feed for suppressing *Salmonella* contamination (Oyofo et al. 1989). Since the decomposition of an abundant naturally occurring D-mannose polymer, β-mannan, requires rigorous conditions, the enzymatic production of D-mannose from other monosaccharides, especially D-glucose, is useful. Isomerization of D-fructose by MI (Hirose et al. 2003; Hu et al. 2016), D-lyxose isomerase (Park et al. 2010a), and L-rhamnose isomerase (Park et al. 2010b) and the epimerization of D-glucose to D-mannose by CE (Park et al. 2011) have been reported to date. The production yield of D-mannose from 200–500 g/L D-fructose through isomerization by the abovementioned isomerases at 45–85°C and pH 7.0–8.0 was 20–35% (molar ratio). As D-fructose is produced from D-glucose by enzymatic isomerization at 60°C and pH 6.0–8.0 using D-xylose isomerase, at approximately 40% yield (molar ratio; Bhosale et al. 1996), the production yield of D-mannose from D-glucose through two-step isomerization, is estimated to be 8–14% (molar ratio). In fact, that of D-mannose by the coupling reaction of D-xylose isomerase and D-lyxose isomerase with 400 g/L D-glucose at 55°C and pH 6.5 was reported to be 16% (Huang et al. 2018). In D-mannose production from 500 g/L D-glucose at 75°C and pH 7.5 by *C. saccharolyticus* CE, the yield of D-mannose from D-glucose was only 15% (molar ratio) due to its isomerization activity (yield of D-fructose was 9.5%) (Park et al. 2011). Isomerization activity was not detected in MEs under the analytical

conditions, and the production yield of D-mannose from 500 g/L D-glucose at 50°C and pH 8.0 by ME (23–24%, molar ratio) was higher than that observed for the reactions previously reported. Thus, ME is a useful biocatalyst for enzymatic D-mannose production, and further study of ME for application in D-mannose production could provide a new and efficient synthetic pathway for D-mannose.

Acknowledgments

We thank Dr. Eri Fukushi of the GC-MS & NMR Laboratory, Research Faculty of Agriculture, Hokkaido University for NMR data analysis; Mr. Yusuke Takada of the DNA sequencing facility of the Research Faculty of Agriculture, Hokkaido University for assistance with DNA sequence analysis; and Ms. Nozomi Takeda of the Global Facility Center, Hokkaido University for the amino acid analysis. We would like to thank Editage (www.editage.jp) for English language editing.

Compliance with ethical standards

Funding: This work was supported in part by a Grant-in-Aid for Scientific Research (C) from the Ministry of Education, Culture, Sports, Science, and Technology of Japan [grant number 18K05382].

Conflict of interest: The authors declare that they have no conflict of interest.

Ethical approval: This article does not contain any studies with human participants or animals performed by any of the authors.

References

Bhosale SH, Rao MB, Deshpande VV (1996) Molecular and industrial aspects of glucose isomerase. Microbiol Rev 60:280-300.

Chen FE, Zhao JF, Xiong FJ, Xie B, Zhang P (2007) An improved synthesis of a key intermediate for (+)-biotin from D-mannose. Carbohydr Res 342:2461-2464. doi: 10.1016/j.carres.2007.06.029

de Lonlay P, Seta N (2009) The clinical spectrum of phosphomannose isomerase deficiency, with an evaluation of mannose treatment for CDG-Ib. Biochim Biophys Acta 1792:841-843. doi: 10.1016/j.bbadis.2008.11.012

Denger K, Weiss M, Felux AK, Schneider A, Mayer C, Spiteller D, Huhn T, Cook AM, Schleheck D (2014) Sulphoglycolysis in *Escherichia coli* K-12 closes a gap in the biogeochemical sulphur cycle. Nature 507:114-117. doi: 10.1038/nature12947

Fujiwara T, Saburi W, Inoue S, Mori H, Matsui H, Tanaka I, Yao M (2013) Crystal structure of *Ruminococcus albus* cellobiose 2-epimerase: structural insights into epimerization of unmodified sugar. FEBS Lett 587:840-846. doi: 10.1016/j.febslet.2013.02.007

Fujiwara T, Saburi W, Matsui H, Mori H, Yao M (2014) Structural insights into the epimerization of β-1,4-linked oligosaccharides catalyzed by cellobiose 2-epimerase, the sole enzyme epimerizing non-anomeric hydroxyl groups of unmodified sugars. J Biol Chem 289:3405-3415. doi: 10.1074/jbc.M113.531251

Ghoreishi SM, Shahrestani RG (2009) Innovative strategies for engineering mannitol production. Trends Food Sci Tech 20:263-270. doi: 10.1016/j.tifs.2009.03.006

Hirose J, Kinoshita Y, Fukuyama S, Hayashi S, Yokoi H, Takasaki Y (2003) Continuous isomerization of D-fructose to D-mannose by immobilized *Agrobacterium radiobacter* cells. Biotechnol Lett 25:349-352.

401 doi: 10.1023/A:1022301725817

402 Hu X, Zhang P, Miao M, Zhang T, Jiang B (2016) Development of a recombinant D-mannose isomerase
403 and its characterizations for D-mannose synthesis. Int J Biol Macromol 89:328-335. doi:
404 10.1016/j.ijbiomac.2016.04.083

405 Huang J, Yu L, Zhang W, Zhang T, Guang C, Mu W (2018) Production of D-mannose from D-glucose by
406 co-expression of D-glucose isomerase and D-lyxose isomerase in *Escherichia coli*. J Sci Food Agric
407 98:4895-4902. doi: 10.1002/jsfa.9021

408 Iida T, Hayashi N, Yamada T, Yoshikawa Y, Miyazato S, Kishimoto Y, Okuma K, Tokuda M, Izumori K
409 (2010) Failure of D-psicose absorbed in the small intestine to metabolize into energy and its low large
410 intestinal fermentability in humans. Metabolism 59:206-214. doi: 10.1016/j.metabol.2009.07.018

411 Ito S, Taguchi H, Hamada S, Kawauchi S, Ito H, Senoura T, Watanabe J, Nishimukai M, Ito S, Matsui H
412 (2008) Enzymatic properties of cellobiose 2-epimerase from *Ruminococcus albus* and the synthesis of rare
413 oligosaccharides by the enzyme. Appl Microbiol Biotechnol 79:433-441. doi: 10.1007/s00253-008-1449-
414 7

415 Itoh T, Mikami B, Hashimoto W, Murata K (2008) Crystal structure of YihS in complex with D-mannose:
416 structural annotation of *Escherichia coli* and *Salmonella enterica yihS*-encoded proteins to an aldose-ketose
417 isomerase. J Mol Biol 377:1443-1459. doi: 10.1016/j.jmb.2008.01.090

418 Itoh T, Mikami B, Maru I, Ohta Y, Hashimoto W, Murata K (2000) Crystal structure of *N*-acyl-D-
419 glucosamine 2-epimerase from porcine kidney at 2.0 Å resolution. J Mol Biol 303:733-744. doi:
420 10.1006/jmbi.2000.4188

Kasumi T, Mori S, Kaneko S, Matsumoto H, Kobayashi Y, Koyama Y (2014) Characterization of mannose isomerase from a cellulolytic actinobacteria *Thermobifida fusca* MBL10003. J Appl Glycosci 61:21-25. doi: 10.5458/jag.jag.JAG-2013_008

Katoh K, Rozewicki J, Yamada KD (2017) MAFFT online service: multiple sequence alignment, interactive sequence choice and visualization. Brief Bioinform. doi: 10.1093/bib/bbx108

Kawahara R, Saburi W, Odaka R, Taguchi H, Ito S, Mori H, Matsui H (2012) Metabolic mechanism of mannan in a ruminal bacterium, *Ruminococcus albus*, involving two mannoside phosphorylases and cellobiose 2-epimerase. Discovery of a new carbohydrate phosphorylase, β-1,4-mannooligosaccharide phosphorylase. J Biol Chem 287:42389-42399. doi: 10.1074/jbc.M112.390336

Kiyohara M, Tachizawa A, Nishimoto M, Kitaoaka M, Ashida H, Yamamoto K. (2009) Prebiotic effect of lacto-*N*-biose I on bifidobacterial growth. Biosci Biotechnol Biochem 73:1175-1179. doi: 10.1271/bbb.80697

Kranjčec B, Papeš D, Altarac S (2014) D-mannose powder for prophylaxis of recurrent urinary tract infections in women: a randomized clinical trial. World J Urol 32:79-84. doi: 10.1007/s00345-013-1091-6

Kuyper M, Winkler AA, van Dijken JP, Pronk JT (2004) Minimal metabolic engineering of *Saccharomyces cerevisiae* for efficient anaerobic xylose fermentation: a proof of principle. FEMS Yeast Res 4:655-664. doi: 10.1016/j.femsyr.2004.01.003

Lee YC, Wu HM, Chang YN, Wang WC, Hsu WH (2007) The central cavity from the (alpha/alpha)$_6$ barrel structure of *Anabaena* sp. CH1 *N*-acetyl-D-glucosamine 2-epimerase contains two key histidine residues for reversible conversion. J Mol Biol 367:895-908. doi: 10.1016/j.jmb.2006.11.001

441 Murakami Y, Ojima-Kato T, Saburi W, Mori H, Matsui H, Tanabe S, Suzuki T (2015) Supplemental
442 epilactose prevents metabolic disorders through uncoupling protein-1 induction in the skeletal muscle of
443 mice fed high-fat diets. Br J Nutr 114:1774-1783. doi: 10.1017/S0007114515003505
444 Nishimoto M, Kitaoka M (2007) Practical preparation of lacto-*N*-biose I, a candidate for the bifidus factor
445 in human milk. Biosci Biotechnol Biochem 71:2101-2104. doi: 10.1271/bbb.70320
446 Nishimukai M, Watanabe J, Taguchi H, Senoura T, Hamada S, Matsui H, Yamamoto T, Wasaki J, Hara H,
447 Ito S (2008) Effects of epilactose on calcium absorption and serum lipid metabolism in rats. J Agric Food
448 Chem 56:10340-10345. doi: 10.1021/jf801556m
449 Ochiai M, Nakanishi Y, Yamada T, Iida T, Matsuo T (2013) Inhibition by dietary D-psicose of body fat
450 accumulation in adult rats fed a high-sucrose diet. Biosci Biotechnol Biochem 77:1123-1126. doi:
451 10.1271/bbb.130019
452 Ochiai M, Onishi K, Yamada T, Iida T, Matsuo T (2014) D-Psicose increases energy expenditure and
453 decreases body fat accumulation in rats fed a high-sucrose diet. Int J Food Sci Nutr 65:245-250. doi:
454 10.3109/09637486.2013.845653
455 Oyofo BA, DeLoach JR, Corrier DE, Norman JO, Ziprin RL, Mollenhauer HH (1989) Prevention of
456 *Salmonella typhimurium* colonization of broilers with D-mannose. Poult Sci 68:1357-1360. doi:
457 10.3382/ps.0681357
458 Park CS, Kim JE, Choi JG, Oh DK (2011) Characterization of a recombinant cellobiose 2-epimerase from
459 *Caldicellulosiruptor saccharolyticus* and its application in the production of mannose from glucose. Appl
460 Microbiol Biotechnol 92:1187-1196. doi: 10.1007/s00253-011-3403-3

461 Park CS, Kwon HJ, Yeom SJ, Oh DK (2010a) Mannose production from fructose by free and immobilized
462 D-lyxose isomerases from *Providencia stuartii*. Biotechnol Lett 32:1305-1309. doi: 10.1007/s10529-010-
463 0300-2
464 Park CS, Yeom SJ, Lim YR, Kim YS, Oh DK (2010b) Characterization of a recombinant thermostable L-
465 rhamnose isomerase from *Thermotoga maritima* ATCC 43589 and its application in the production of L-
466 lyxose and L-mannose. Biotechnol Lett 32:1947-1953. doi: 10.1007/s10529-010-0385-7
467 Ranta K, Nieminen K, Ekholm FS, Poláková M, Roslund MU, Saloranta T, Leino R, Savolainen J (2012)
468 Evaluation of immunostimulatory activities of synthetic mannose- containing structures mimicking the β-
469 (1→2)-linked cell wall mannans of *Candida albicans.* Clin Vaccine Immunol 19:1889-1893. doi:
470 10.1128/CVI.00298-12
471 Saburi W (2016) Functions, structures, and applications of cellobiose 2-epimerase and glycoside hydrolase
472 family 130 mannoside phosphorylases. Biosci Biotechnol Biochem 80:1294-1305. doi:
473 10.1080/09168451.2016.1166934
474 Saburi W, Jaito N, Kato K, Tanaka Y, Yao M, Mori H (2018) Biochemical and structural characterization
475 of *Marinomonas mediterranea* D-mannose isomerase Marme_2490 phylogenetically distant from known
476 enzymes. Biochimie 144:63-73. doi: 10.1016/j.biochi.2017.10.016
477 Saburi W, Tanaka Y, Muto H, Inoue S, Odaka R, Nishimoto M, Kitaoka M, Mori H (2015) Functional
478 reassignment of *Cellvibrio vulgaris* EpiA to cellobiose 2-epimerase and an evaluation of the biochemical
479 functions of the 4-*O*-β-D-mannosyl-D-glucose phosphorylase-like protein, UnkA. Biosci Biotechnol
480 Biochem 79:969-977. doi: 10.1080/09168451.2015.1012146

481 Saburi W, Yamamoto T, Taguchi H, Hamada S, Matsui H (2010) Practical preparation of epilactose
482 produced with cellobiose 2-epimerase from *Ruminococcus albus* NE1. Biosci Biotechnol Biochem
483 74:1736-1737. doi: 10.1271/bbb.100353
484 Schägger H, Cramer WA, von Jagow G (1994) Analysis of molecular masses and oligomeric states of
485 protein complexes by blue native electrophoresis and isolation of membrane protein complexes by two-
486 dimensional native electrophoresis. Anal Biochem 217:220–230. doi: 10.1006/abio.1994.1112
487 Standley DM, Toh H, Nakamura H (2007) ASH structure alignment package: Sensitivity and selectivity in
488 domain classification. BMC Bioinformatics 8:116. doi: 10.1186/1471-2105-8-116
489 Suzuki T, Nishimukai M, Shinoki A, Taguchi H, Fukiya S, Yokota A, Saburi W, Yamamoto T, Hara H,
490 Matsui H (2010a) Ingestion of epilactose, a non-digestible disaccharide, improves postgastrectomy
491 osteopenia and anemia in rats through the promotion of intestinal calcium and iron absorption. J Agric Food
492 Chem 58:10787-10792. doi: 10.1021/jf102563y
493 Suzuki T, Nishimukai M, Takechi M, Taguchi H, Hamada S, Yokota A, Ito S, Hara H, Matsui H (2010b)
494 The nondigestible disaccharide epilactose increases paracellular Ca absorption via rho-associated kinase-
495 and myosin light chain kinase-dependent mechanisms in rat small intestines. J Agric Food Chem 58:1927-
496 1932. doi: 10.1021/jf9035063
497 Takeshita K, Suga A, Takada G, Izumori K (2000) Mass production of D-psicose from D-fructose by a
498 continuous bioreactor system using immobilized D-tagatose 3-epimerase. J Biosci Bioeng 90:453-455. doi:
499 10.1016/S1389-1723(01)80018-9
500 Watanabe J, Nishimukai M, Taguchi H, Senoura T, Hamada S, Matsui H, Yamamoto T, Wasaki J, Hara H,

Ito S (2008) Prebiotic properties of epilactose. J Dairy Sci 91:4518-4526. doi: 10.3168/jds.2008-1367

Figure caption

Fig. 1 Phylogenetic analysis of AGE superfamily proteins

Proteins of functionally known AGE superfamily enzymes are presented. AGE, acylglucosamine 2-epimerase; CE, cellobiose 2-epimerase; MI, D-mannose isomerase; and SQI, sulfoquinovose isomerase.

Fig. 2 SDS-PAGE and BN-PAGE of Runsl_4512 and Dfer_5652

Recombinant Runsl_4512 and Dfer_5652, purified from *E. coli* transformant, were analyzed on SDS-PAGE and BN-PAGE. Lane M, R, and D indicate molecular mass standard, Runsl_4512, and Dfer_5652.

Fig. 3 TLC analysis of the reaction products by Runsl_4512 and Dfer_5652

Plus and minus lanes indicate the reactions with and without the enzyme, respectively. A, Runsl_4512; B, Dfer_5652.

Fig. 4 The s-*v* plot for D-mannose epimerization by Runsl_4512 and Dfer_5652

Close and open circles indicate Runsl_4512 and Dfer_5652, respectively. Values and error bars are average and standard deviation of three independent experiments.

Fig. 5 Time course of production of D-mannose from D-glucose

Black circle, D-glucose; white circle, D-mannose; and black triangle, D-fructose. Values indicate mean ± standard deviation for three independent experiments.

Fig. 6 NMR analysis of ME reaction products

Time course of the ME reaction was monitored using ^{1}H-NMR. A, reaction with mixture of α-D-mannose and β-D-mannose; B, reaction with mixture of α-D-glucose and β-D-glucose; C, reaction with α-D-glucose; and D, reaction with β-D-glucose. Reaction time (min) is presented on the left side of the figures. E, ^{1}H-NMR and ^{2}H-NMR of equilibrated reaction mixture of ME. The spectrum of the equimolar mixture of D-glucose and D-mannose (Man + Glc) is shown as standard.

Fig. 7 Multiple sequence alignment of AGE superfamily enzymes

Multiple sequence alignment was performed using MAFTFFTash (Standley et al. 2007). The secondary structure is depicted above the sequence. Amino acid residues involved in substrate binding (reducing end part of disaccharides in CE) are presented in bold face. Catalytic His residues are indicated by black circles. Asp187 of Runsl_4512 and Dfer_5652 is indicated by black triangle. RaCE, *Ruminococcus albus* CE; RmCE, *Rhodothermus marinus* CE; MmMI, *Marinomonas mediterranea* MI; TfMI, *Thermobifida fusca* MI; EsSQI, *Escherichia coli* SQI; and AspAGE, *Anabaena* sp. AGE.

Fig. 8 Predicted reaction mechanism of ME

Arrows indicate electron transfer processes that convert β-D-mannose to β-D-glucose. The bond between 2-C and 3-C would rotate after acceptance of a proton from the general acid catalyst, His404, in the epimerization of D-mannose, according to the reaction mechanism of CE (Fujiwara et al. 2014).

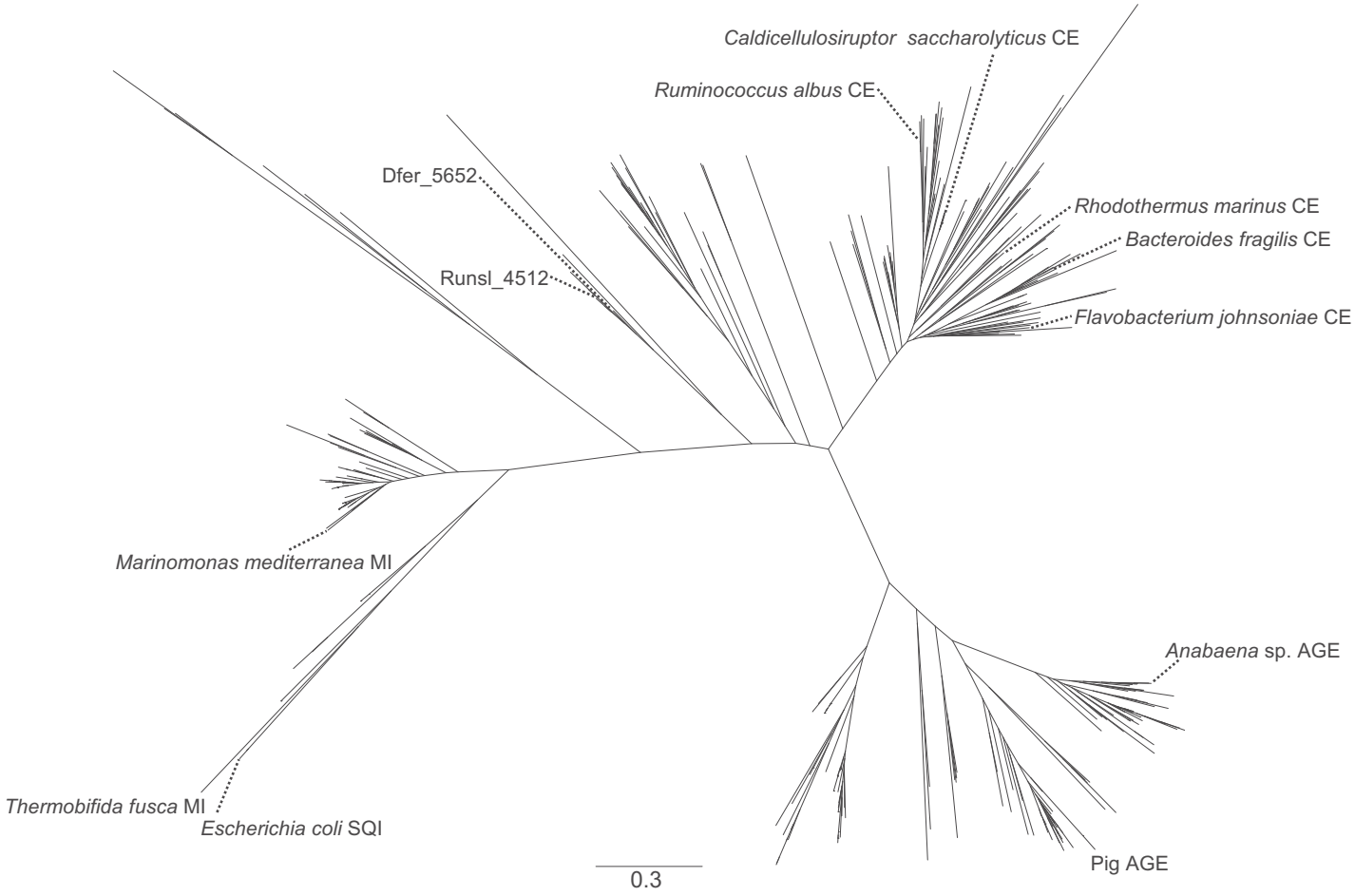

Fig. 1, Saburi et al.

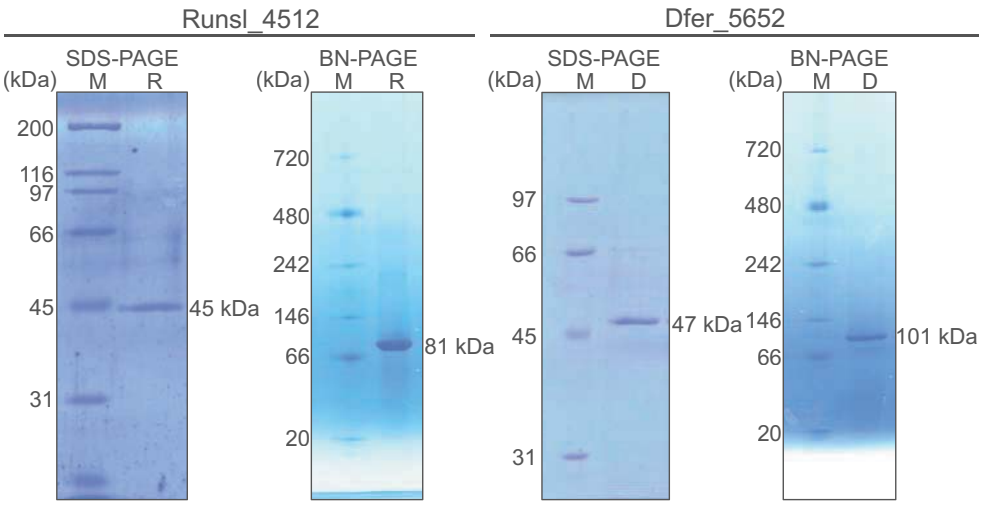

Fig. 2., Saburi et al.

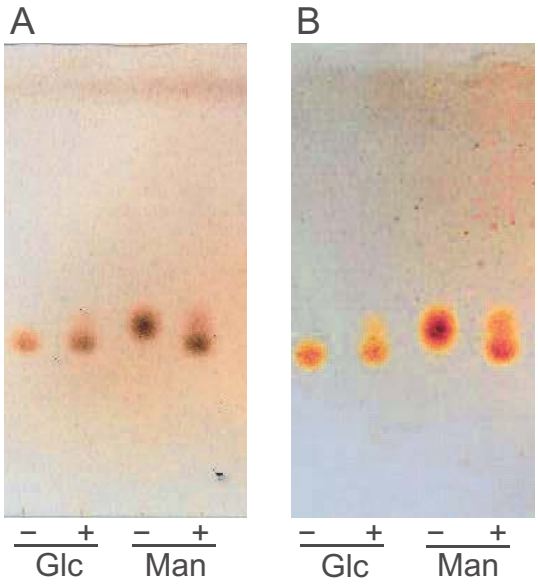

Fig. 3., Saburi et al.

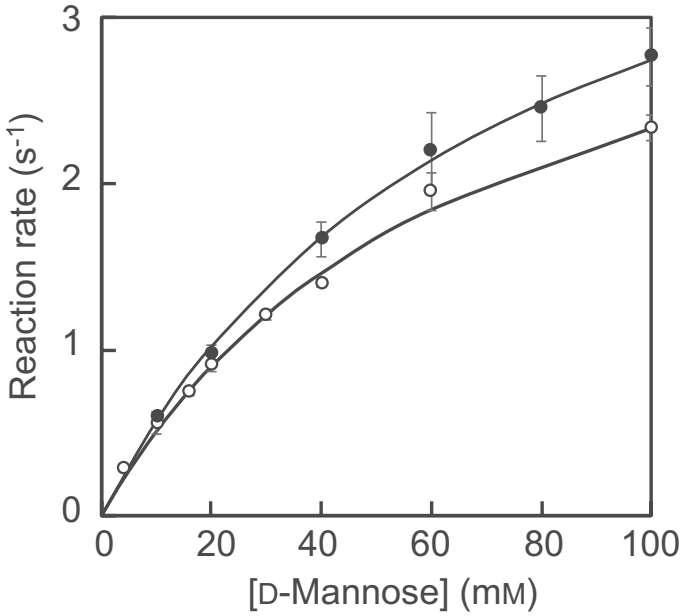

Fig. 4., Saburi et al.

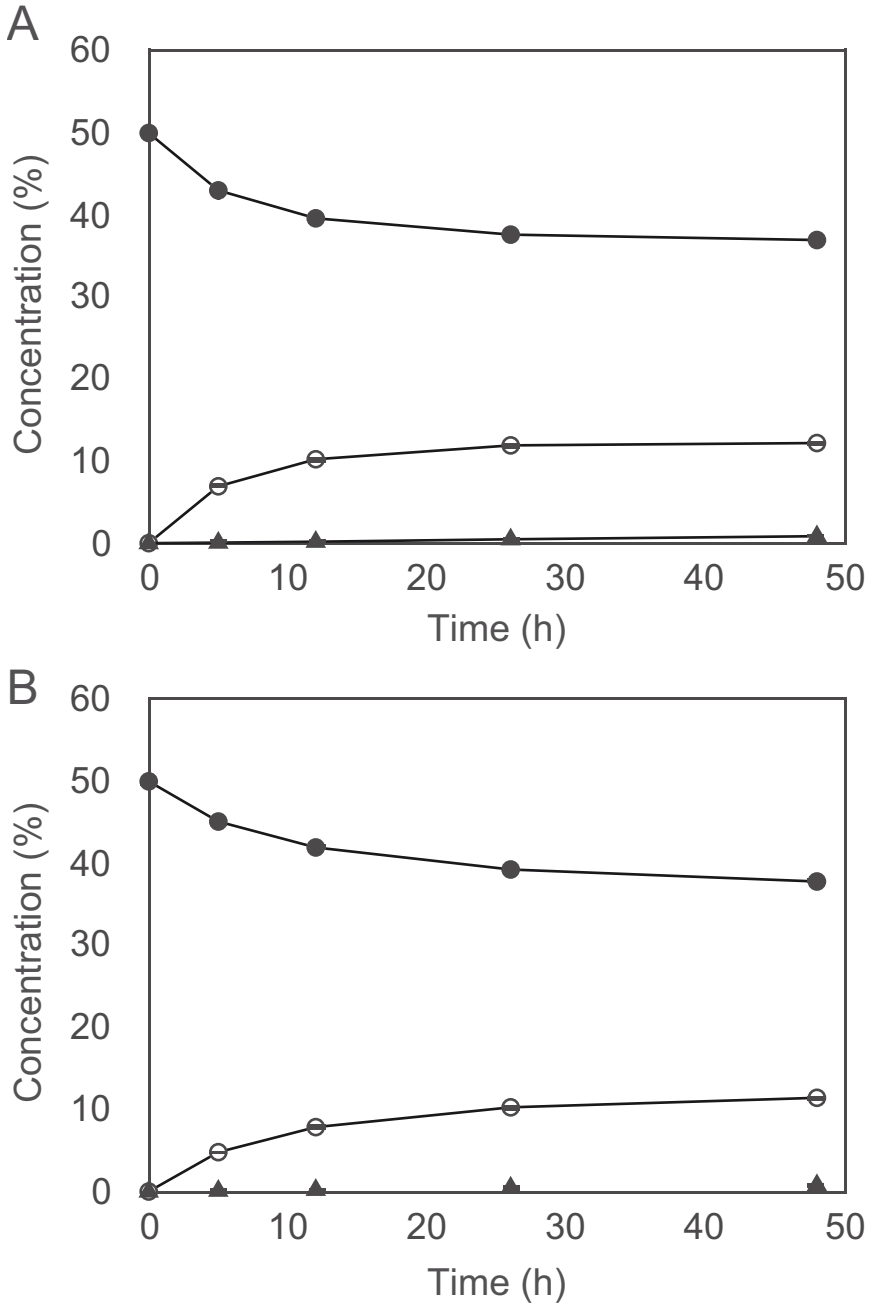

Fig. 5., Saburi et al.

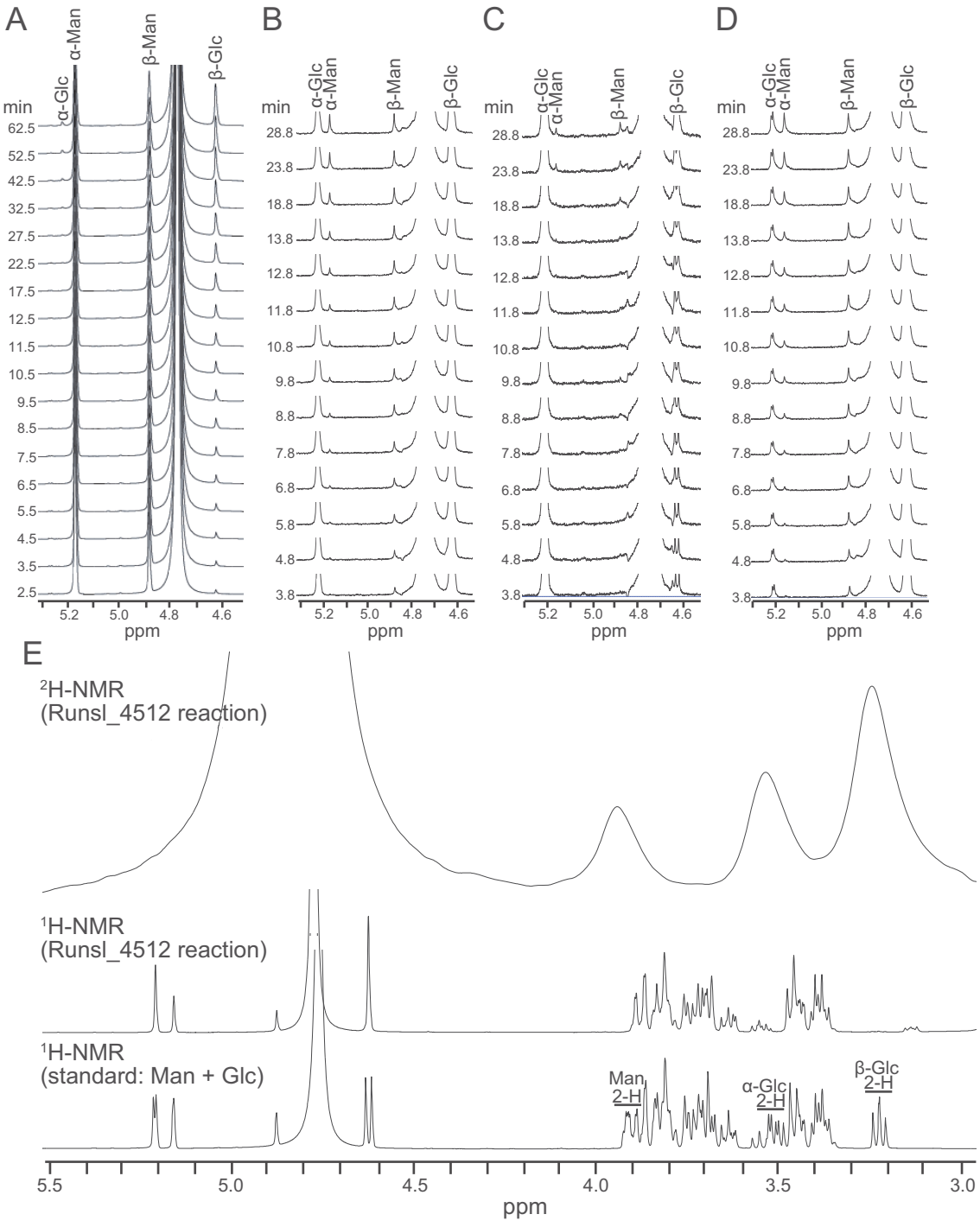

Fig. 6. Saburi et al.

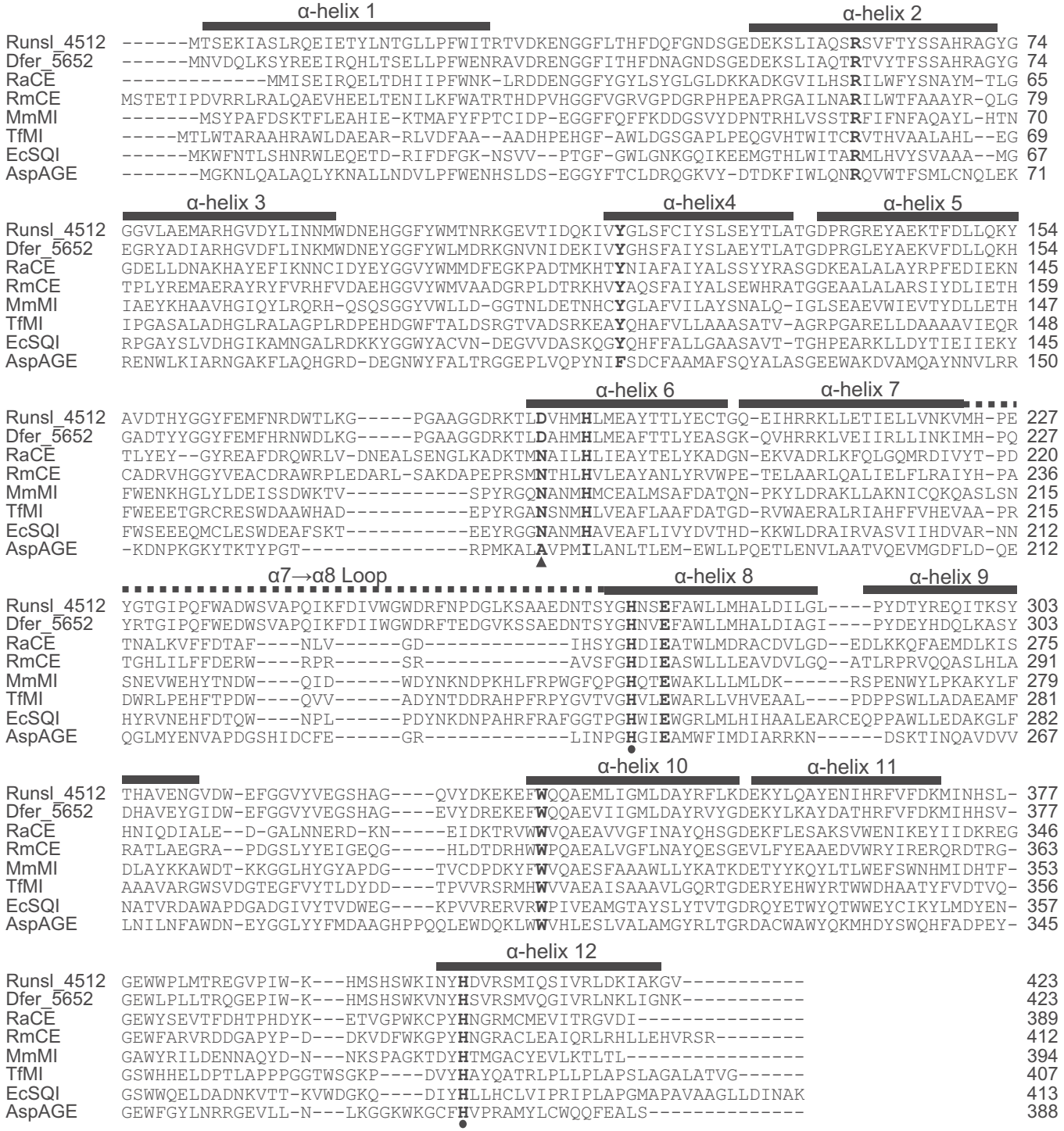

Fig. 7., Saburi et al.

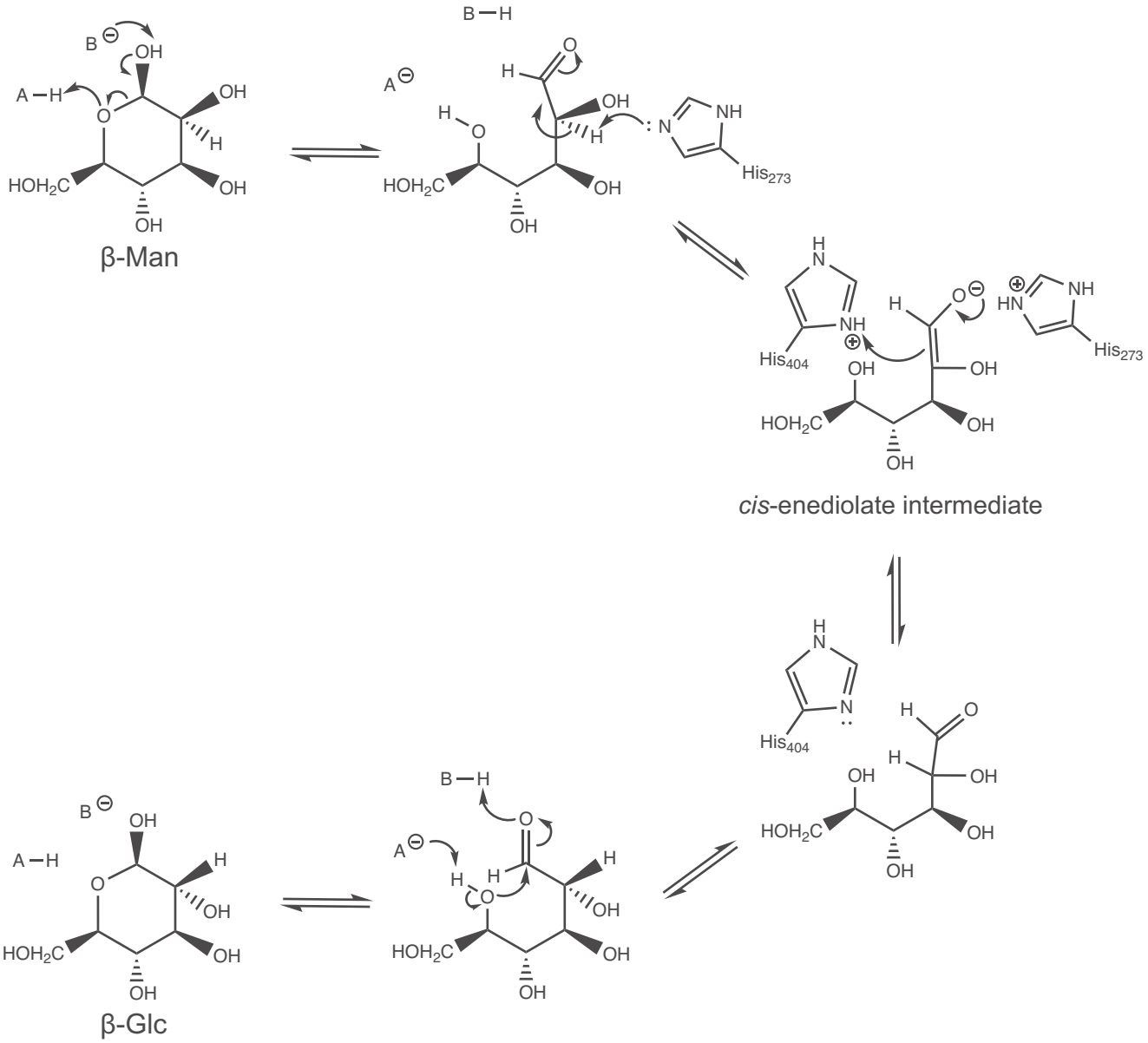

Fig. 8., Saburi et al.

Table 1. Sequences of primers used in this study.

Name	Sequence (5′ to 3′)	Purpose
Runsl_4512_s	TATATTTTTCATATGACTTCTGAAAAAATT	Preparation of expression plasmid
Runsl_4512_a	AAATTATTCCTCGAGCACCCCTTTTGCAAT	Preparation of expression plasmid
Dfer_5652_s	CCATATTTTGAATTCATGAATGTAGATCAA	Preparation of expression plasmid
Dfer_5652_a	TCCAAATTCCTCGAGCTTATTTCCAATCAG	Preparation of expression plasmid
D187N_s	ACCCTC**A**A**T**GTACACATGCACCTCATG	Mutagenesis in Runsl_4512
D187N_a	GTGTAC**A**T**T**GAGGGTCTTGCGGTCACC	Mutagenesis in Runsl_4512

Recognition sites of restriction endonucleases are underlined. Substituted nucleotides are shown in bold face.

Table 2. Kinetic parameters of Runsl_4512 and Dfer_5652 for D-mannose.

Enzyme	k_{cat} (min^{-1})	K_m (mM)	k_{cat}/ K_m (min^{-1} mM^{-1})
Runsl_4512	286 ± 20	73.5 ± 6.7	3.89
Dfer_5652	233 ± 25	66.4 ± 11.1	3.51
CsCE	44.3 ± 0.6	51.8 ± 1.2	0.855
CvCE	6.78 ± 0.18	245 ± 10	0.0277

Values are mean ± standard deviation for three independent experiments. CsCE, *Caldicellulosiruptor saccharolyticus* CE (Park et al. 2011); CvCE, *Cellvibrio vulgaris* CE (Saburi et al. 2015).